N-terminal arginylation generates a bimodal degron that modulates autophagic proteolysis

Young Dong Yoo[a,1], Su Ran Mun[a,1], Chang Hoon Ji[a], Ki Woon Sung[a], Keum Young Kang[a], Ah Jung Heo[a], Su Hyun Lee[a], Jee Young An[b], Joonsung Hwang[c], Xiang-Qun Xie[d,e,f,g,h], Aaron Ciechanover[a,i,2], Bo Yeon Kim[c,2], and Yong Tae Kwon[a,j,2]

[a]Protein Metabolism Medical Research Center and Department of Biomedical Sciences, College of Medicine, Seoul National University, Jongno-gu, 03080 Seoul, Korea; [b]Center for Genome Engineering, Institute for Basic Science, Yuseong-gu, 34126 Daejeon, Korea; [c]Anticancer Agent Research Center, Korea Research Institute of Bioscience and Biotechnology (KRIBB), 28116 Cheongju, Korea; [d]Department of Pharmaceutical Sciences and Computational Chemical Genomics Screening Center, School of Pharmacy, University of Pittsburgh, Pittsburgh, PA 15260; [e]National Center of Excellence for Computational Drug Abuse Research, University of Pittsburgh, Pittsburgh, PA 15260; [f]Drug Discovery Institute, University of Pittsburgh, Pittsburgh, PA 15260; [g]Department of Computational Biology, School of Medicine, University of Pittsburgh, Pittsburgh, PA 15260; [h]Department of Structural Biology, School of Medicine, University of Pittsburgh, Pittsburgh, PA 15260; [i]Technion Integrated Cancer Center, Faculty of Medicine, Technion-Israel Institute of Technology, 31096 Haifa, Israel; and [j]Ischemic/Hypoxic Disease Institute, College of Medicine, Seoul National University, Jongno-gu, 03080 Seoul, Korea

Contributed by Aaron Ciechanover, February 2, 2018 (sent for review November 6, 2017; reviewed by Zvulun Elazar, Anna Kashina, and David C. Rubinsztein)

The conjugation of amino acids to the protein N termini is universally observed in eukaryotes and prokaryotes, yet its functions remain poorly understood. In eukaryotes, the amino acid L-arginine (L-Arg) is conjugated to N-terminal Asp (Nt-Asp), Glu, Gln, Asn, and Cys, directly or associated with posttranslational modifications. Following Nt-arginylation, the Nt-Arg is recognized by UBR boxes of N-recognins such as UBR1, UBR2, UBR4/p600, and UBR5/EDD, leading to substrate ubiquitination and proteasomal degradation via the N-end rule pathway. It has been a mystery, however, why studies for the past five decades identified only a handful of Nt-arginylated substrates in mammals, although five of 20 principal amino acids are eligible for arginylation. Here, we show that the Nt-Arg functions as a bimodal degron that directs substrates to either the ubiquitin (Ub)-proteasome system (UPS) or macroautophagy depending on physiological states. In normal conditions, the arginylated forms of proteolytic cleavage products, D^{101}-CDC6 and D^{1156}-BRCA1, are targeted to UBR box-containing N-recognins and degraded by the proteasome. However, when proteostasis by the UPS is perturbed, their Nt-Arg redirects these otherwise cellular wastes to macroautophagy through its binding to the ZZ domain of the autophagic adaptor p62/STQSM/Sequestosome-1. Upon binding to the Nt-Arg, p62 acts as an autophagic N-recognin that undergoes self-polymerization, facilitating cargo collection and lysosomal degradation of p62–cargo complexes. A chemical mimic of Nt-Arg redirects Ub-conjugated substrates from the UPS to macroautophagy and promotes their lysosomal degradation. Our results suggest that the Nt-Arg proteome of arginylated proteins contributes to reprogramming global proteolytic flux under stresses.

N-end rule pathway | ATE1 R-transferase | ubiquitin-proteasome system | macroautophagy | p62/STQSM/Sequestosome-1

Eukaryotic cells operate two major proteolytic systems, the ubiquitin (Ub)-proteasome system (UPS) and autophagy. In the UPS, substrates are conjugated with Ub and degraded through the proteasome into short peptides (1). In protein quality control, terminally misfolded proteins are fed to the UPS or autophagy for destruction (2). In principle, soluble substrates are ubiquitinated by E3 ligases and degraded by the proteasome (1). However, when misfolded substrates excessively accumulate beyond the UPS's capacity, Ub-conjugated cargoes are redirected to macroautophagy and segregated by autophagosomes for lysosomal degradation (3). The delivery of cargoes to autophagy involves specific receptors such as p62, which recognizes Ub chains using its Ub association domain (4). Cargo-loaded p62 undergoes self-polymerization, forming condensed cargo–p62 complexes, which are delivered to phagophores through interaction with LC3. To date, little is known about how autophagy is modulated in response to accumulating cargoes.

The conjugation of amino acids to the protein N termini by aminoacyl-tRNA transferases (EC2.3.2) is universal in both eukaryotes and prokaryotes, yet its biological meaning is poorly understood (5). In eukaryotes, L-Arg is conjugated to the N-terminal (Nt)-Asp and Nt-Glu by *ATE1*-encoded Arg-tRNA transferases (R-transferases; EC 2.3.2) (6). Nt-arginylation also occurs on Nt-Asn and Nt-Gln following deamidation into Nt-Asp and Nt-Glu or on Nt-Cys following oxidation into Cys sulfinic acid ($CysO_2$) or Cys sulfonic acid ($CysO_3$) (5). The functions of Nt-arginylation include proteolysis through the N-end rule pathway, wherein a single N-terminal residue acts as an N-degron. Known N-degrons include Arg, Lys, His (type 1, positively charged), Trp, Phe, Tyr, Leu, and Ile (type 2, bulky hydrophobic) (5). These degrons are recognized by N-recognins that facilitate substrate degradation. In mammals, the Nt-Arg is

Significance

Conjugation of the amino acid L-arginine (L-Arg) to the protein N termini is a universal posttranslational modification in eukaryotes, yet its functions remain poorly understood. Previous studies showed that the N-terminal Arg of arginylated substrates is bound by N-recognins to induce substrate ubiquitination and proteasomal degradation via the N-end rule pathway of the ubiquitin (Ub)-proteasome system (UPS). Here, we show that the same Nt-Arg residues of arginylated proteins modulate proteolytic flux via macroautophagy when misfolded proteins accumulate beyond the UPS's capacity. Their Nt-Arg residues bind and allosterically activate the autophagic adaptor p62/STQSM/Sequestosome-1, facilitating cargo collection and lysosomal degradation. Our results suggest that the Nt-Arg proteome of arginylated proteins contributes to reprogramming global proteolytic flux when the UPS is in trouble.

Author contributions: Y.D.Y., S.R.M., C.H.J., K.W.S., and J.Y.A. designed research; Y.D.Y., S.R.M., C.H.J., K.W.S., K.Y.K., A.J.H., S.H.L., and J.Y.A. performed research; X.-Q.X. contributed new reagents/analytic tools; Y.D.Y., S.R.M., C.H.J., K.W.S., K.Y.K., S.H.L., J.Y.A., J.H., A.C., and B.Y.K. analyzed data; and Y.D.Y., S.R.M., and Y.T.K. wrote the paper.

Reviewers: Z.E., Weizmann Institute of Science; A.K., University of Pennsylvania School of Veterinary Medicine; and D.C.R., University of Cambridge.

Conflict of interest statement: Y.T.K., D.C.R., and Z.E. are coauthors on a 2016 *Autophagy Guidelines* publication that lists more than 1,000 authors who published their work in *Autophagy*.

[1]Y.D.Y. and S.R.M. contributed equally to this work.

[2]To whom correspondence may be addressed. Email: aaroncie@technion.ac.il, bykim@kribb.re.kr, or yok5@snu.ac.kr.

This article contains supporting information online at www.pnas.org/lookup/suppl/doi:10.1073/pnas.1719110115/-/DCSupplemental.

Published online March 5, 2018.

recognized by UBR boxes of N-recognins such as UBR1, UBR2, UBR4/p600, and/or UBR5/EDD (7). Upon binding to Nt-Arg, these N-recognins promote substrate ubiquitination and proteasomal degradation of short-lived regulators via the UPS (5).

The Nt-Arg can be exposed following cleavage by endopeptidases or enzymatically generated through the modification of Nt-Asn, Nt-Gln, Nt-Cys, Nt-Asp, and Nt-Glu (8). The human genome encodes more than 600 endopeptidases (9), including caspases and calpains that cleave more than 2,000 substrates (10). Approximately one-third of human proteins are destined to the Golgi-secretory pathway and cleaved at their signal peptides during translocation into the endoplasmic reticulum (ER) (4). These endopeptidases generate a large number of proteolytic cleavage products constitutively or in a manner induced by stresses. To date, there are no known principles underlying the metabolic fates of proteolytic cleavage products. One such principle is the N-end rule which, in principle, links the identity of P1′ residues (i.e., the N-terminal residues of endoproteolytic cleavage products) to substrates' metabolic stability (11). Indeed, the P1′ residues of many substrates of calpains and caspases are conserved as destabilizing or arginylation-permissive amino acids of the N-end rule (12, 13). Overall, the functions of the P1′ residues generated on endoproteolytic cleavage products remain unclear.

Studies by us and others have shown that a set of ER-residing proteins are Nt-arginylated, including BiP/GRP78, calreticulin (CRT), and protein disulfide isomerase (PDI) (4, 14). Their Nt-arginylation is induced by cytosolic double-stranded DNA as an indication of an invading DNA-containing pathogen in innate immunity. Nt-arginylated BiP (R-BiP) accumulates in the cytosol, where its Nt-Arg binds the ZZ domain of p62. An in vitro assay showed that the dipeptide Arg-Ala facilitated the self-polymerization of p62 and the interaction of p62 with LC3 (4). To date, the physiological meaning of the interaction of R-BiP with p62 remains largely unknown.

In this study, we show that the Nt-Arg of arginylated proteins functions as a bimodal degron that distributes substrates to either the UPS or autophagy as part of protein quality control. In normal conditions, the Nt-Arg of arginylated substrates is recognized by the UBR box of UBR proteins for degradation through the UPS. However, if proteolytic flux via the UPS is compromised, the Nt-Arg of the same substrates is preferentially recognized by the ZZ domain of p62, facilitating p62 self-polymerization, autophagosome biogenesis, and lysosomal degradation of autophagic protein cargoes. Our results suggest that Nt-arginylation contributes to reprogramming of proteolytic flux under stresses.

Results

Caspase-Generated CDC6$^{101–562}$ Is Arginylated at Nt-Asp101 and Degraded via the UPS. We previously screened the substrates of the N-end rule pathway using genome-wide functional proteomics, in which ∼14,000 proteins were individually expressed in rabbit reticulocyte lysates and allowed ubiquitination in the presence of N-end rule inhibitors (15). Here, we characterized the 66-kDa replication licensing factor CDC6 as a putative substrate of Nt-arginylation. Mouse CDC6 contains a caspase 3-binding motif, LVFD$^{97–100}$, whose cleavage generates 52-kDa CDC6$^{101–562}$ bearing the arginylation-permissive Nt-Asp101. Sequence alignment showed that both the caspase-binding motif and Nt-arginylation permissiveness of P1′ residue are evolutionarily conserved (Fig. 1*A*). We therefore determined whether CDC6$^{101–562}$ (D^{101}-CDC6) is an N-end rule substrate by expressing the fusion protein Ub-X^{101}–CDC6 (X = D, V, or RD) whose cotranslational cleavage by deubiquitination enzymes generates Ub and X^{101}-CDC6 (Fig. S1*A*). Immunoblotting and cycloheximide degradation assays showed that D^{101}-CDC6 was short-lived and metabolically stabilized by the proteasome inhibitor MG132 (Fig. 1 *B* and *C*) through the destabilizing activity of its Nt-Asp101. In these assays, the permanently arginylated form of CDC6$^{101–562}$, R-CDC6, was normally degraded in ATE1-deficient cells (Fig. 1*E*). Thus, CDC6$^{101–562}$ is degraded by the proteasome through the activity of Nt-Asp101 as a degradation determinant.

To validate that CDC6$^{101–562}$ is arginylated, we raised R-CDC6 antibody that exclusively recognizes arginylated CDC6 using the

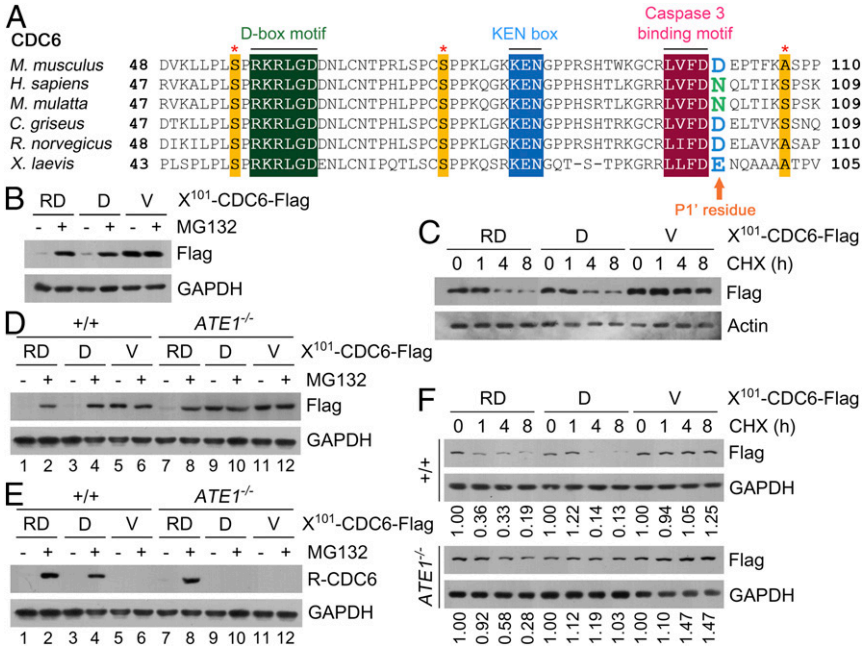

Fig. 1. Arginylated CDC6$^{101–562}$ is normally degraded via the UPS-linked N-end rule pathway. (*A*) Sequence alignment of caspase 3-binding motifs of CDC6 proteins. (*B*) HeLa cells expressing X^{101}-CDC6 (X = D, V, or RD) were treated with 10 μM MG132 for 5 h, followed by immunoblotting. (*C*) Cycloheximide degradation assay. HeLa cells expressing X^{101}-CDC6-Flag were treated with 10 μM cycloheximide (CHX). (*D* and *E*) Same assay as *B* in $^{+/+}$ and *ATE1*$^{-/-}$ MEFs. The GAPDH panel in *E* is identical to that in *D*. CDC6 was detected using anti-Flag in *D* and anti–R-CDC6 in *E*. (*F*) CHX degradation assay in $^{+/+}$ and *ATE1*$^{-/-}$ MEFs.

peptide R-D^{101}EPTFKASPP (Fig. S1 *B* and *C*). Immunoblotting analysis using R-CDC6 antibody showed that overexpressed CDC6 was cleaved into an expected 52-kDa fragment when treated with etoposide (Fig. S1*D*). CDC6 was not cleaved when Asp100 of the caspase cleavage sequence LVFD$^{97–100}$ was mutated to Ala (Fig. S1 *D* and *E*) or cells were treated with the caspase 3 inhibitor Z-DEVD-FMK (Fig. S1*F*). The 52-kDa band was degraded in a manner sensitive to MG132 (Fig. S1*D*, lane 10 vs. lane 9). Thus, caspase-generated CDC6$^{101–562}$ is arginylated at Nt-Asp101 and degraded through the UPS.

We next determined the role of ATE1 in Nt-arginylation of D^{101}-CDC6. In vivo degradation assays showed that D^{101}-CDC6 was degraded in $^{+/+}$ mouse embryonic fibroblasts (MEFs) but stabilized in *ATE1*$^{-/-}$ MEFs [Fig. 1 *D* (lane 9 vs. lane 3) and *F*], resulting in the accumulation of its unarginylated form (Fig. 1 *D* and *E*, lane 3 vs. lane 9). The ability of *ATE1*$^{-/-}$ MEFs to arginylate and degrade CDC6$^{101–562}$ was restored by overexpressed ATE1 (Fig. S1*G*). Thus, ATE1-mediated arginylation of CDC6$^{101–562}$ facilitates proteasomal degradation.

Arginylated CDC6$^{101–562}$ Is Normally Degraded via the UPS-Linked N-End Rule Pathway. N-degrons in the UPS-linked N-end rule pathway are recognized by N-recognins such as UBR1, UBR2, UBR4, and UBR5 (8). Immunoblotting analysis showed that D^{101}-CDC6 was markedly stabilized in *UBR1*$^{-/-}$*UBR2*$^{-/-}$ MEFs compared with $^{+/+}$ MEFs (Fig. S1*H*). Metabolic stabilization of R^{101}-CDC6 required the loss of three N-recognins: UBR1, UBR2, and UBR4 (Fig. S1*H*). To measure the in vivo half-life of D^{101}-CDC6, we labeled newly synthesized CDC6 using ^{35}S-Met/Cys and chased its decay. D^{101}-CDC6 was rapidly degraded through the destabilizing activity of Nt-Asp101 (Fig. S1 *I* and *J*). In addition, D^{101}-CDC6 was almost completely stabilized in *ATE1*$^{-/-}$ or *UBR1*$^{-/-}$*UBR2*$^{-/-}$*UBR4*^{RNAi} MEFs (Fig. S1 *I* and *J*). These results suggest that R-CDC6$^{101–562}$ is degraded by the UPS-linked N-end rule pathway via the ATE1-UBR1/UBR2/UBR4 circuit.

It has been shown that CDC6 carries the D-box (nos. 47–52) and KEN box (nos. 72–74) and is degraded through ubiquitination by the anaphase-promoting complex/cyclosome (APC/C) during normal cell cycle (16) (Fig. 1*A*). Our results suggest that during apoptotic induction, the cleavage by caspase 3 removes the APC/C degron and generates an N-degron, leading to proteolysis by the N-end rule pathway (Fig. S1*K*). Thus, CDC6 can be dually modulated by two distinct E3 systems.

Arginylated CDC6$^{101–562}$ Is Targeted to Autophagy Under Proteasomal Inhibition. Immunoblotting analysis of cells treated with 1 μM MG132 for 17 h showed that RD^{101}-CDC6 accumulated when autophagy was inhibited by hydroxychloroquine (HCQ) (Fig. 2*A*).

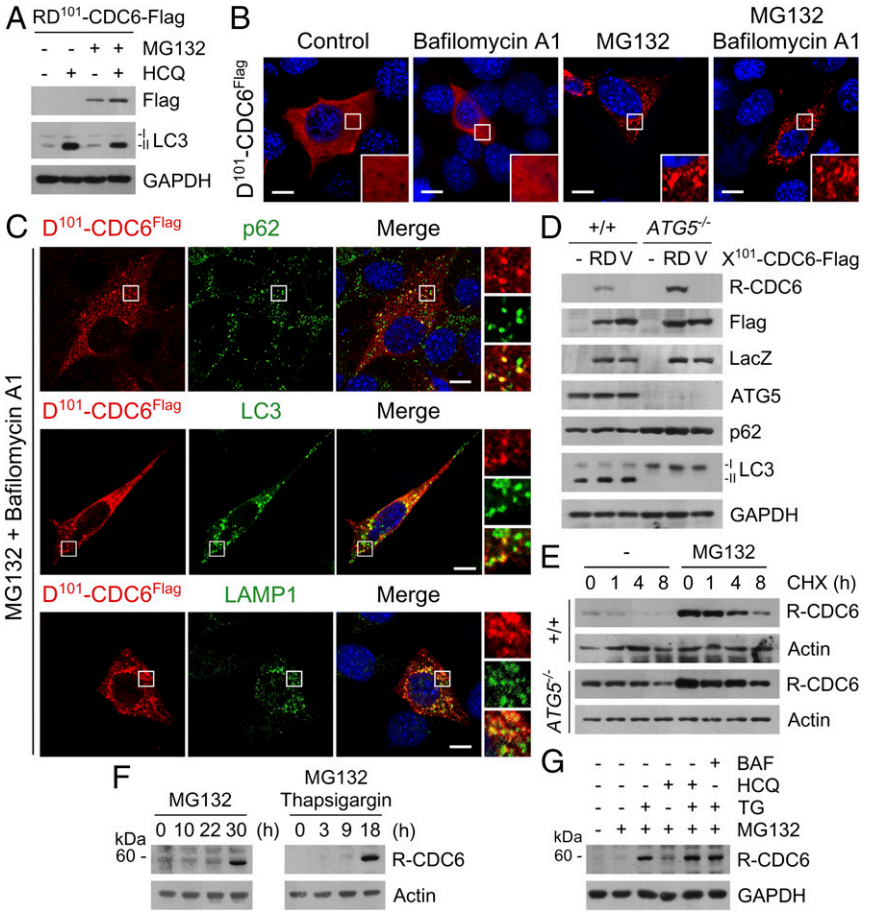

Fig. 2. Arginylated CDC6$^{101–562}$ is degraded via autophagy under proteasomal inhibition. (*A*) HEK293 cells expressing RD^{101}-CDC6-Flag were treated with 3 μM MG132 and 25 μM HCQ for 17 h. (*B*) MEFs expressing D^{101}-CDC6-Flag were treated with 0.3 μM MG132 for 17 h alone or together with 0.2 μM BAF for 5 h, followed by anti-Flag immunostaining. (Scale bars, 10 μm.) (*C*) Same as *B*, followed by immunostaining of p62, LC3, or LAMP1. (Scale bars, 10 μm.) (*D*) Wild-type and *ATG5*$^{-/-}$ MEFs expressing X^{101}-CDC6-Flag (X = V or RD) were subjected to immunoblotting analysis. (*E*) Wild-type and *ATG5*$^{-/-}$ MEFs expressing RD^{101}-CDC6-Flag were treated with 1 μM cycloheximide (CHX) alone or together with 10 μM MG132, followed by immunoblotting. (*F*) HeLa cells were treated with MG132 alone or together with thapsigargin. (*G*) HeLa cells were treated with 3 μM MG132 singly or in combination with 0.2 μM BAF, 25 μM HCQ, and/or 0.2 μM thapsigargin (TG) for 17 h, followed by immunoblotting.

Metabolically stabilized RD^{101}-CDC6 formed cytosolic puncta that became more prominent upon autophagic inhibition (Fig. 2*B*). Approximately 50% of CDC6 puncta were positive for the autophagic adaptor p62 (Fig. 2*C*). Quantitation of these puncta suggested that at least 50% of CDC6 and p62 was delivered to $LC3^+$ autophagosomes and, subsequently, $LAMP1^+$ lysosomes (Fig. 2*C*). An immunoblotting-based in vivo degradation assay showed that autophagic degradation of RD^{101}-CDC6 was significantly inhibited in $ATG5^{-/-}$ MEFs (Fig. 2 *D* and *E*). Thus, under proteasomal inhibition, a subpopulation of D^{101}-CDC6 becomes a substrate of p62-dependent autophagy for lysosomal degradation.

Next, we validated these results using endogenous CDC6. Immunoblotting analysis using R-CDC6 antibody showed that HeLa cells under proteasomal inhibition generated endogenous RD^{101}-CDC6, with a size of 52 kDa (Fig. 2*F*). RD^{101}-CDC6 was synergistically generated when cotreated with the ER stressor thapsigargin or the autophagic blocker HCQ (Fig. 2 *F* and *G* and Fig. S2*A*). Immunostaining analysis using R-CDC6 antibody detected endogenous D^{101}-CDC6 signals as cytosolic puncta (Fig. S2*B*), which colocalized with p62 and LC3 as well as LAMP1 puncta (Fig. S2*C*). These results suggest that under proteasomal inhibition, RD^{101}-CDC6 is redirected from proteasomal flux to autophagic flux via p62.

The Nt-Arg of RD^{101}-CDC6 Is an Autophagic N-Degron. To determine whether the Nt-Arg of RD^{101}-CDC6 acts as an autophagic N-degron, we examined its localization using immunostaining analysis. In contrast to $^{+/+}$ MEFs, D^{101}-CDC6 failed to form cytosolic puncta in $ATE1^{-/-}$ MEFs (Figs. S2 *D* and *E* and S3–S5), which was validated using endogenous D^{101}-CDC6 (Fig. S1*C*). In addition, the mutation of Nt-Asp^{101} to Val abolished the ability to form cytosolic puncta (Fig. S2 *D* and *E*) and to colocalize with p62 (Fig. S3), LC3 (Fig. S4), and LAMP1 (Fig. S5). In all these assays, RD^{101}-CDC6 was targeted to autophagy independent of ATE1 (Figs. S2 *D* and *E* and S3–S5). These results suggest that Nt-arginylation generates a bimodal degron that directs D^{101}-CDC6 to the UPS or autophagy.

Nt-Arginylated D-$CDC6^{101-562}$ Binds p62 and Induces Its Self-Polymerization. We recently showed that the Nt-arginylated form of the ER chaperone BiP, R-BiP, binds p62 and induces its self-oligomerization (4). To determine whether RD^{101}-CDC6 binds and activates p62, we mixed HEK293 cell extracts with a 12-mer peptide corresponding to its N-terminal region (Fig. 3*A*). The RD^{101}-CDC6 peptide readily pulled down endogenous p62 (Fig. 3*B*). In contrast, no such binding was observed with D^{101}-CDC6 or V^{101}-CDC6 peptides (Fig. 3*B*), suggesting that RD^{101}-CDC6 binds p62 through Nt-Arg. As an alternative assay, immunoprecipitation confirmed that RD^{101}-CDC6 binds p62 and that their interaction was enhanced when autophagic flux was blocked (Fig. S6*B*). Next, we determined the Nt-Arg–binding site of p62. Our previous study showed that the Nt-Arg of a model N-end rule substrate bound the ZZ domain of p62 (17), a structural and functional homolog of UBR boxes of N-recognins (Fig. S6*A*). Consistently, X-peptide pulldown assays showed that the interaction between RD^{101}-CDC6 and p62 was disrupted by Ala mutation of two zinc-coordinating Cys residues, Cys142 and Cys145 (Fig. 3*C*), as well as other conserved resides in the ZZ domain (Fig. S6*C*). These results suggest that RD^{101}-CDC6 binds to the p62 ZZ domain through the N-end rule interaction of its Nt-Arg. Consistent with these in vitro binding assays, D^{101}-CDC6 was not delivered to autophagy in $p62^{-/-}$ MEFs, as determined by the formation of cytosolic puncta (Fig. 3*D*). The autophagic targeting of D^{101}-CDC6 was restored when p62 was ectopically expressed in $p62^{-/-}$ MEFs (Fig. S6*D*). Thus, RD^{101}-CDC6 is targeted to autophagy through its interaction with p62.

To determine whether the binding of RD^{101}-CDC6 to the p62 ZZ domain activates the function of p62, we performed in vitro aggregation assays (4). We mixed HEK293 cell extracts expressing p62-myc with the pentapeptide R-DEPT corresponding to the N termini of RD^{101}-CDC6 and separated proteins in nonreducing

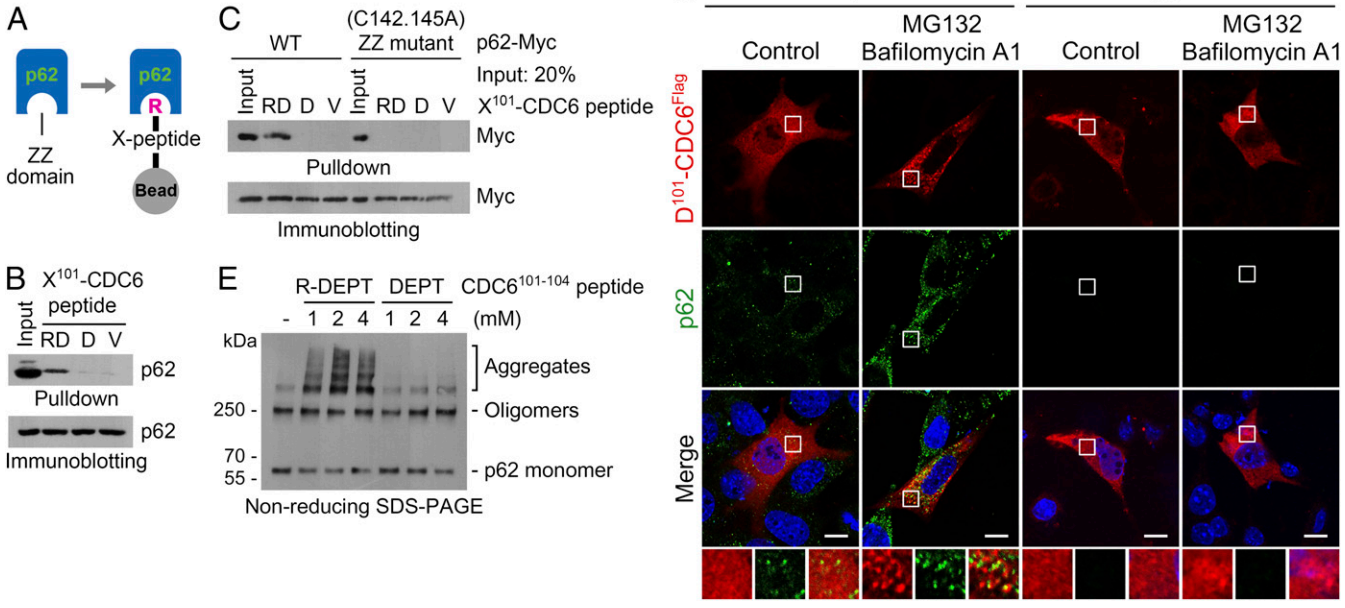

Fig. 3. Arginylated $CDC6^{101-562}$ binds and activates p62. (*A*) Diagram illustrating X-peptide pulldown assay using synthetic peptides. (*B*) HEK293 cell lysates were mixed with X^{101}-CDC6 peptides (X = D, V, or RD), followed by immunoblotting analysis. (*C*) HEK293 cells expressing wild-type or C142/145A p62-myc were subjected to pulldown assay with X^{101}-CDC6 peptides. (*D*) Wild-type and $p62^{-/-}$ MEFs expressing D^{101}-CDC6-Flag were treated with 0.3 μM MG132 for 12 h, followed by cotreatment with 0.2 μM BAF for 5 h, and analyzed using anti-Flag immunostaining in comparison to p62. (Scale bars, 10 μm.) (*E*) HEK293 cell lysates were incubated with the tetrapeptide R-$DEPT^{101-104}$ or $DEPT^{101-104}$ for 2 h, followed by nonreducing SDS/PAGE.

SDS/PAGE lacking β-mercaptoethanol. In contrast to the control peptide, the R-D^{101}EPT peptide readily induced the formation of high-molecular-weight p62 aggregates, which are linked through covalent bonding (Fig. 3*E*). These results suggest that the Nt-Arg of RD^{101}-CDC6 induces the polymerization of p62 during cargo collection in macroautophagy.

Various Cellular Proteins Bind and Active p62 Through Their Nt-Arginylation. During apoptotic induction, caspase 3 cleaves 207-kDa human BRCA1 into 80-kDa $BRCA1^{1156–1863}$ (D^{1156}-BRCA1) bearing Nt-Asp1156, which is known to be degraded by the N-end rule pathway (18, 19). To determine the role of p62 as a receptor for arginylated proteins, we generated antibody-specific to Nt-arginylated D^{1156}-BRAC1 (Fig. S7*A*). In vivo degradation assays showed that D^{1156}-BRCA1 was normally degraded by the proteasome (Fig. 4*A*, lane 4 vs. lane 3) through Nt-arginylation (lane 5 vs. lane 1) of Nt-Asp1156 (Fig. 4*A*, lane 5 vs. lane 3), which was validated using a cycloheximide degradation assay (Fig. 4*B*). Thus, D^{1156}-BRCA1 is Nt-arginylated by ATE1 and degraded through the UPS-linked N-end rule pathway (Fig. 4*A*).

To determine the metabolic fate of D^{1156}-BRCA1 under proteasomal inhibition, we immunostained X^{1156}-BRCA1 (X = D, V, or RD). RD^{1156}-BRCA1 accumulated under proteasome inhibition to form cytosolic puncta (Fig. S7*B*, column 3) through the activity of Nt-Asp1156 (Fig. S7*B*, column 2 vs. column 1). An autophagy flux assay using bafilomycin A1 (BAF) showed that RD^{1156}-BRCA1 puncta were subjected to lysosomal degradation (Fig. S7*B*). Whereas D^{1156}-BRCA1 was not delivered to autophagy in *ATE1*$^{-/-}$ MEFs (Fig. S7*C*), its arginylated form was readily targeted to autophagy independent of ATE1 (Fig. S7*C*). A portion of D^{1156}-BRCA1 puncta were positive for p62 and LC3, as well as for the lysosomal marker LAMP1 (Fig. 4*C* and Fig. S7*D*). Moreover, an X-peptide pulldown assay showed that RD^{1156}-BRCA1 bound p62 through its Nt-Arg (Fig. 4*D*). Thus, D^{1156}-BRCA1 is redirected from the UPS to autophagy through Nt-arginylation under prolonged proteasome inhibition.

Previous studies have identified a number of arginylation substrates in the cytosol (e.g., BRCA1, Aβ42, tau) and the ER [BiP, PDI, CRT (4, 18–20)]. In addition, our bioinformatics analysis predicted that the ER chaperones GRP94 and ERdj5 carry Nt-Asp as a putative N-degron. To generalize our findings, we asked whether other arginylated substrates bind p62 through Nt-Arg. We synthesized 11-mer peptides corresponding to the N termini of the arginylated forms (Fig. 4*E*). Except for the R-GRP94 peptide, all of the arginylated peptides captured endogenous p62 (Fig. 4*F*, lane 1). No such bind-ing was observed with the native peptides (Fig. 4*F*, lane 2 vs. lane 1) or the Nt-Val mutant peptides (Fig. 4*F*, lane 3). These results suggest that p62 is a general receptor of cellular Nt-arginylated proteins.

Nt-Arginylation Is Induced upon Crisis in Proteostasis. To determine whether the autophagic targeting of RD^{101}-CDC6 is induced by excessive misfolded proteins, we treated HEK293 cells with the HSP90 inhibitor geldanamycin, which generates excessive misfolded proteins. The level of RD^{101}-CDC6 was markedly increased by geldanamycin (Fig. 5*A* and Fig. S8*A*). RD^{101}-CDC6 synergistically accumulated when autophagic flux was blocked

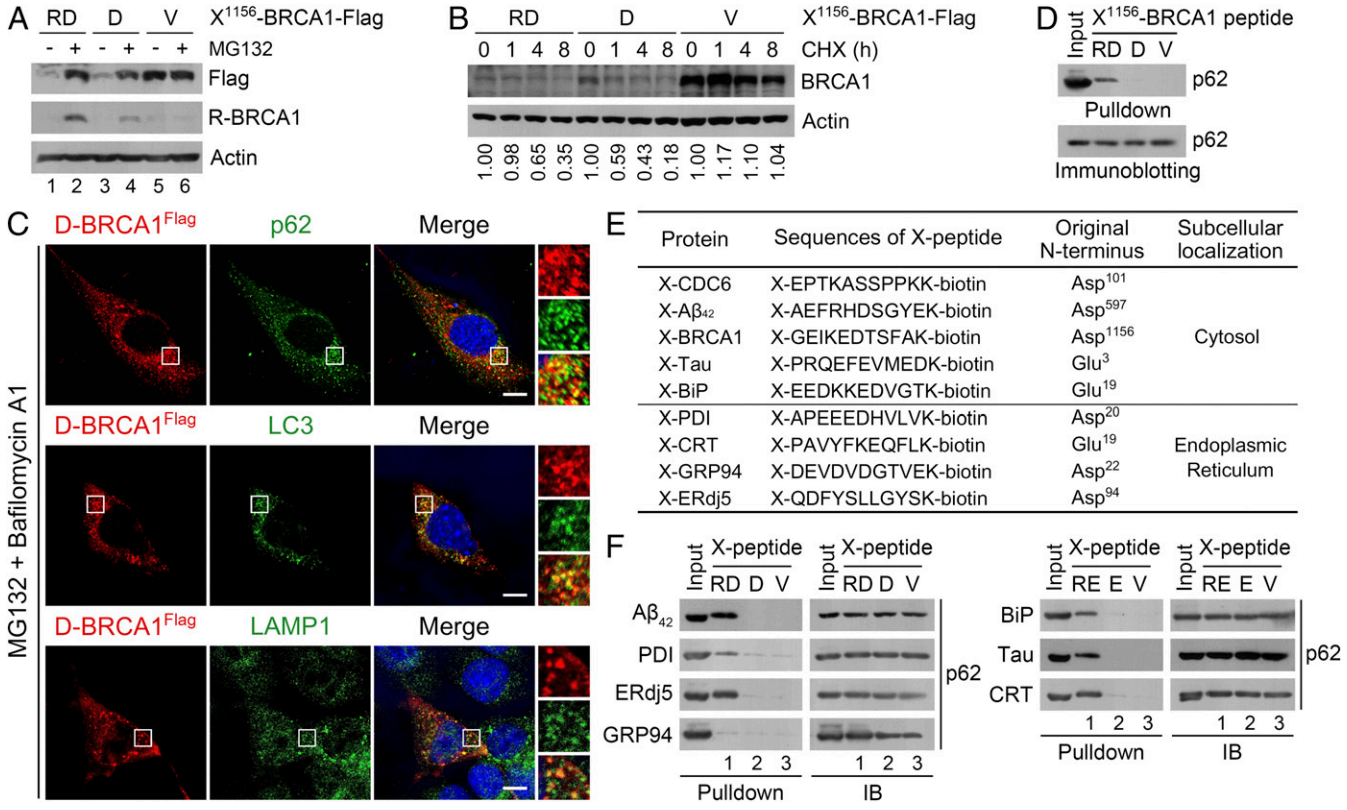

Fig. 4. P62 is a general receptor of cellular Nt-arginylated proteins. (*A*) HeLa cells expressing X^{1156}-BRCA1-Flag (X = D, V, or RD) were treated with 10 μM MG132 for 5 h and immunoblotted. (*B*) HeLa cells expressing X^{1156}-BRCA1-Flag were treated with 10 μM cycloheximide (CHX), followed by immunoblotting. Relative band intensities were normalized to those with no treatment. (*C*) MEFs were treated with 0.3 μM MG132 12 h, followed by cotreatment with 0.2 μM BAF for 5 h, and analyzed using anti-Flag immunostaining in comparison to p62, LC3, and LAMP1. (Scale bars, 10 μm.) (*D*) HEK293 cell lysates were subjected to X-peptide pulldown assay of p62 using X-$BRCA1^{1156–1166}$ peptides. (*E*) Sequences of N-terminal regions of (putative) arginylation substrates used in *F*. (*F*) X-peptides were mixed with HEK293 cell extracts to pulldown p62. IB, immunoblotting.

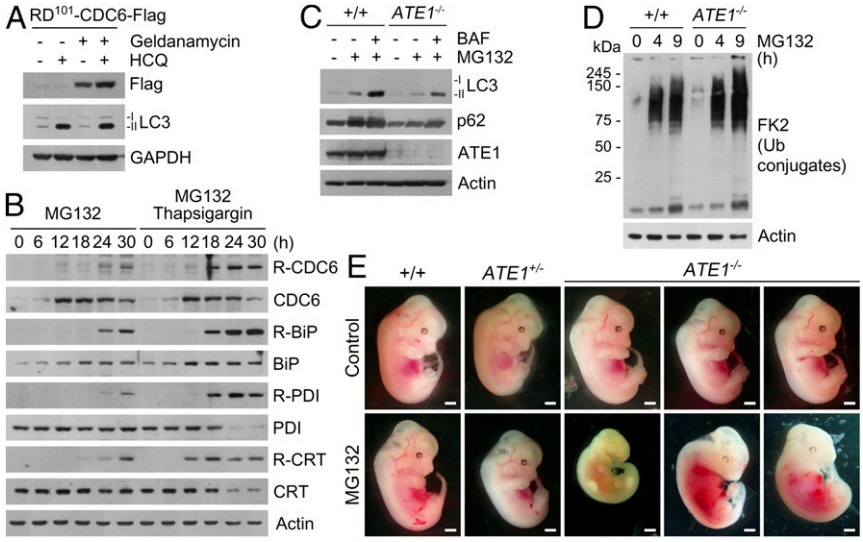

Fig. 5. Nt-arginylation modulates for autophagic proteolysis. (*A*) HEK293 cells expressing X^{101}-CDC6-Flag were treated with 1 μM geldanamycin and 25 μM HCQ for 17 h. (*B*) HeLa cells were treated with 3 μM MG132 alone or together with 0.2 μM thapsigargin. (*C*) Control and *ATE1*$^{-/-}$ MEFs were treated with 0.3 μM MG132 alone for 17 h or, alternatively, for 12 h, followed by cotreatment with 0.2 μM BAF for 5 h. (*D*) Control and *ATE1*$^{-/-}$ MEFs were treated with 0.3 μM MG132 and subjected to immunoblotting, followed by immunoblotting analysis using FK2 antibody specific to Ub conjugates. (*E*) Pregnant *ATE1*$^{+/-}$ female mice were injected i.v. with 20 mg/kg MG132 for 3 d. The resulting embryos and littermate controls at E12.5 were harvested, and their gross morphology was examined. (Scale bars, 1 mm.)

(Fig. 5*A*). Immunostaining analysis showed that geldanamycin-induced D^{101}-CDC6 formed cytosolic puncta positive for p62 as well as LC3 (Fig. S8 *B* and *C*). Thus, D^{101}-CDC6 is redirected from the UPS to autophagy when misfolded proteins excessively accumulate beyond the capacity of the UPS.

Next, we determined whether Nt-arginylation is generally induced under proteasomal inhibition. Immunoblotting analysis using antibodies specific to arginylated forms showed that Nt-arginylation of cytosolic CDC6, as well as the ER chaperones BiP, PDI, and CRT, was coinduced under proteasome inhibition, which involves the accumulation of misfolded proteins (Fig. 5*B*). Immunostaining showed that all of the arginylated proteins formed cytosolic puncta (Fig. S8*D*). These results suggest that Nt-arginylation may occur on a large number of cellular proteins under proteotoxic conditions.

R-Transferases Are Required for Autophagic Protein Quality Control. We determined the role of the Nt-Arg of arginylated substrates in protein quality control. Immunoblotting analysis of cells under proteasomal inhibition showed that *ATE1*$^{-/-}$ MEFs were moderately but significantly impaired in the synthesis and activation of LC3 (Fig. 5*C*), which was restored by ATE1 overexpression (Fig. S8*E*). The failure to induce autophagy correlated to the excessive accumulation of Ub conjugates (Fig. 5*D*). Next, we validated these results in *ATE1*$^{-/-}$ mouse embryos that we have previously shown die around embryonic day (E) 15.5 associated with cardiovascular defects (21). We injected pregnant female mice i.p. ($n = 4$) with 20 mg/kg MG132 for 1, 2, or 3 d starting from E9.5 and harvested the embryos ($n = 28$). Whereas $^{+/+}$ and *ATE1*$^{+/-}$ embryos ($n = 23$) showed no obvious symptoms under all conditions, *ATE1*$^{-/-}$ embryos ($n = 5$) treated for 2–3 d exhibited various abnormalities, such as developmental defects of the forelimbs and cardiovascular system (as indicated by a swollen pericardial sac), leading to precocious death (Fig. 5*E*). These impairments of *ATE1*$^{-/-}$ embryos correlated to the defects in autophagic induction under proteasomal inhibition (Fig. S8*F*). To further address the cytoprotective role of arginylation against proteotoxicity, we treated $^{+/+}$ and *ATE1*$^{-/-}$ MEFs with various stressors and measured their viability based on the activity of mitochondrial NADH dehydrogenase. *ATE1*$^{-/-}$ MEFs were hypersensitive to the inhibition of proteasomal or autophagic flux compared with other types of stresses (Fig. S8*G*). Thus, ATE1 plays a cytoprotective role in autophagic protein proteolysis.

A Chemical Mimic of Nt-Arg Reprograms Proteolytic Flux via Macroautophagy. Based on the interaction of Nt-Arg with the p62 ZZ domain, we recently developed a small molecule ligand, XIE62-1004, to the ZZ domain of p62 (17). Using the chemical mimic, we examined whether the autophagic N-degron Nt-Arg modulates the activity of p62 and autophagic protein quality control. Consistent with our previous observation (17), XIE62-1004 induced the autophagic degradation of p62 and the synthesis of LC3-II (Fig. S9 *A* and *C*), which are associated with the increased formation of $p62^{+}LC3^{+}$ autophagic vacuoles (Fig. S9*B*). Moreover, XIE62-1004 restored the down-regulated level of LC3-II in *ATE1*$^{-/-}$ MEFs to a normal level under proteasomal inhibition (Fig. S9*D*). Next, to validate these results in animals, we injected C57BL/6 mice i.v. with 10 mg/kg XIE62-1004 and killed them after 1, 3, 6, or 24 h. The animals showed a time-course increase in the level of LC3-1 and its conversion to LC3-II (Fig. S9*E*). This increase and activation of LC3 were associated with increased levels of autophagic core components such as ATG3, ATG5, and ATG7 (Fig. S9*E*). When the sections of brains were immunostained, control brains contained the basal levels of $p62^{+}$ and $LC3^{+}$ puncta, the majority of which were mutually exclusive of each other, indicating that macroautophagy is in an inactive state (Fig. 6*A*). By contrast, XIE62-1004 markedly induced the formation of $p62^{+}LC3^{+}$ cytosolic puncta (Fig. 6*A*). These results provide in vivo evidence that the Nt-Arg of cellular arginylated proteins induces p62-dependent macroautophagy.

We asked whether XIE62-1004 facilitates the targeting of misfolded proteins to autophagy. Immunoblotting analysis showed that cells treated with XIE62-1004 contained low levels of Ub conjugates under proteasomal inhibition (Fig. 6*B*). When HeLa cells were cotreated with BAF and MG132, XIE62-1004 facilitated the formation of $Ub^{+}LC3^{+}$ puncta (Fig. 6*C* and Fig. S9*F*). These results suggest that XIE62-1004 facilitates the delivery of

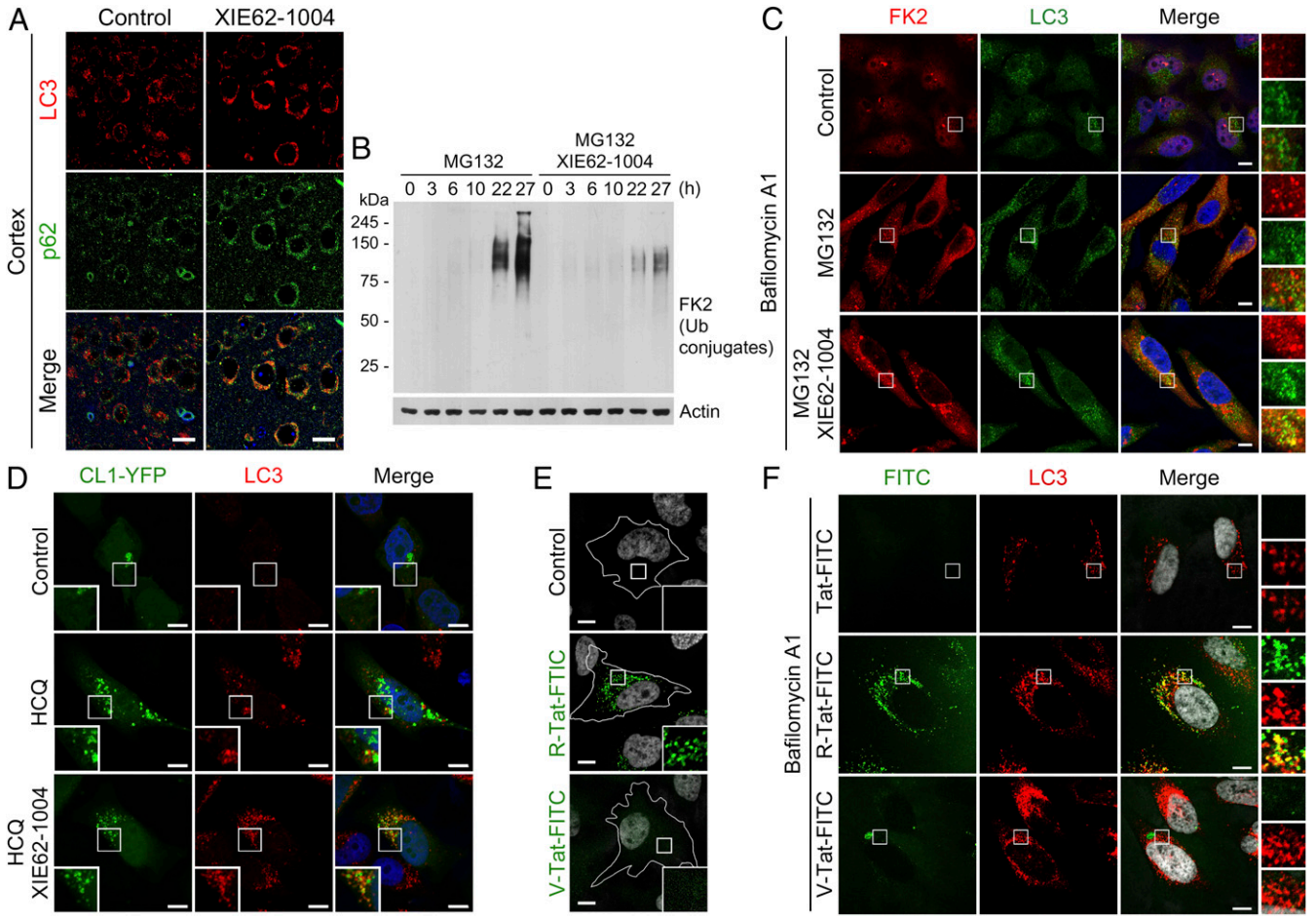

Fig. 6. Chemical mimicry of Nt-Arg activates autophagy and facilitates autophagic targeting of misfolded proteins. (*A*) C57BL/6 mice were injected i.v. with 10 mg/kg XIE62-1004. Brains were harvested 24 h after treatment, paraffin-sectioned, and immunostained for LC3 and p62. Shown are cortex areas. (Scale bars, 10 μm.) (*B*) HeLa cells were treated with 3 μM MG132 alone or together with 10 μM XIE62-1004 for indicated times, followed by immunoblotting analysis of Ub conjugates. (*C*) HeLa cells were treated with 3 μM MG132 alone or together with 10 μM XIE62-1004 for 12 h, followed by cotreatment with 0.2 μM BAF for 5 h and immunostaining with FK2 and LC3 antibodies. (Scale bars, 10 μm.) (*D*) HeLa cells expressing CL1-YFP were treated with 25 μM HCQ alone or in combination with 10 μM XIE62-1004 for 17 h, followed by immunostaining analysis of LC3. (Scale bars, 10 μm.) (*E*) HeLa cells were incubated with 25 μM X-TAT-FITC (X = R or V) peptide for 18 h, followed by FITC fluorescence analysis. (Scale bars, 10 μm.) (*F*) HeLa cells were incubated with native TAT-FITC or X-TAT-FITC (X = R or V) for 8 h, followed by cotreatment with 0.1 μM BAF for 4 h and immunostaining analysis of LC3 in comparison to FITC fluorescence. (Scale bars, 10 μm.)

Ub-tagged misfolded proteins to autophagosomes. Next, to further support this finding, we monitored the distribution and degradation of the model substrate CL1-YFP, which is spontaneously misfolded and forms cytosolic aggregates (22). Immunostaining analysis showed that CL1-YFP accumulated as cytosolic puncta when autophagic flux was blocked by HCQ (Fig. 6*D*). Some CL1-YFP puncta colocalized with $LC3^+$ autophagic vacuoles. Notably, the XIE62-1004 treatment facilitated the delivery of CL1-YFP into autophagic flux, as evidenced by drastically increased colocalization with $LC3^+$ puncta (Fig. 6*D*). These results suggest that the Nt-Arg of arginylated proteins modulates the delivery of misfolded proteins to autophagosomes and their degradation.

Synthetic Peptides Bearing the Nt-Arg Are Targeted to Autophagy via p62. To test whether the Nt-Arg residues of cellular arginylated proteins form an N-proteome that is targeted to autophagy, we synthesized a cell-penetrating peptide carrying Nt-Arg. An 11-mer peptide derived from HIV-1 transactivator of transcription (Tat) protein (23) was N-terminally conjugated with L-Arg and C-terminally conjugated with FITC. The resulting peptide, R-Tat-FITC, was introduced into HeLa cells, followed by fluorescence and immunostaining analyses. R-Tat-FITC readily formed cytosolic puncta in a dose- and time-dependent manner (Fig. 6*E* and Fig. S10*A*). The majority of R-Tat-$FITC^+$ puncta colocalized with p62 (Fig. S10*B*) and LC3 (Fig. 6*F* and Fig. S10*C*) puncta. In contrast, no autophagic targeting was observed with the same peptide lacking Nt-Arg or when Nt-Arg was changed to Val. Triple-immunostaining analysis showed that R-Tat peptide induced the formation of $TAT^+p62^+LC3^+$ cytosolic puncta, which was abolished when the Nt-Arg of Tat peptide was changed to Val (Fig. S10*D*). These results suggest that the Nt-Arg of arginylated proteins are targeted to and, possibly, modulate p62-dependent macroautophagy under stresses.

Discussion

In this study, we show that Nt-arginylation generates a bimodal degron for the UPS and autophagy through the N-end rule pathway (Fig. 7). In this cross-talk, the Nt-Arg normally functions as a degron that promotes ubiquitination of short-lived substrates by UBR box-containing N-recognins, leading to proteasomal degradation (Fig. 7 *A* and *B*). Our results suggest that when misfolded proteins excessively accumulate, the protein N termini act as an autophagic delivery determinant and degron, as well as an activity-modulating ligand (Fig. 7*C*). Through this

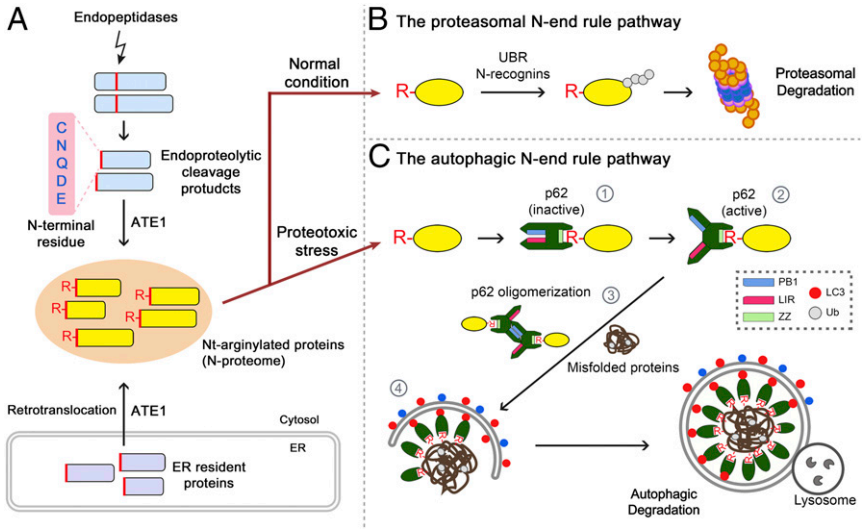

Fig. 7. Hypothetical model illustrating the role of Nt-arginylation as a bimodal degron that modulates the cross-talk between the UPS and autophagy. (*A*) In eukaryotic cells, large numbers of cleavage products are generated by exopeptidases and endopeptidases. (*B*) Some of them are Nt-arginylated, and thus are normally degraded through ubiquitination via the UPS-linked N-end rule pathway. (*C*) However, when Nt-arginylated substrates cannot be properly processed by the proteasome under cellular stresses, they are metabolically stabilized, possibly associated with reduced activities of N-end rule machinery, resulting in increased concentrations of the Nt-Arg. The Nt-Arg of arginylated substrates from various subcellular compartments, such as the cytosol and ER, forms an N-proteome that directly binds the ZZ domain of p62 (step 1). The binding induces self-polymerization of p62 through a conformational change from a closed configuration to an open configuration (step 2), facilitating the collection of cargoes such as misfolded proteins and their aggregates (step 3) and, thus accelerating the delivery of p62–cargo complexes to autophagosomes (step 4). Through this mechanism, cells can sense and react to accumulating autophagic cargoes by activating p62 in a timely fashion using otherwise protein "wastes."

functional reprogramming, arginylated substrates are no longer wastes but form a unique proteome that modulates autophagic proteolysis. Together with our earlier findings of R-BiP (4), our results provide an autophagy-modulating mechanism composed of several steps (Fig. 7*C*): (*i*) The Nt-Arg residues of cellular arginylated proteins bind to the ZZ domain of p62 (step 1); (*ii*) the binding induces an allosteric conformational change of p62, exposing its PB1 and LIR domains (step 2) (*iii*); the Nt-Arg interaction induces p62 self-polymerization, and thus its activity as an autophagic adaptor, facilitating the collection and coaggregation of cargoes such as misfolded proteins (step 3); and (*iv*) the Nt-Arg also induces the interaction of p62 with LC3 anchored on autophagic membranes, promoting the targeting of p62–cargo complexes along with arginylated substrates (step 4). Through this mechanism, Nt-arginylated substrates, normally destined to waste management by the proteasome, contribute to reprogramming proteolytic flux under stresses.

The human genome expresses more than 600 proteases representing over 2% of the proteome. They generate a large number of proteolytic cleavage products bearing the Nt-Arg or arginylation-permissive residues. The expression and activity of some proteases are enhanced under stresses that involve the misregulation of proteostasis such as ER stress, oxidative stress, and proteasomal inhibition (24). Overall, these diverse types of proteolytic cleavage products generate a pool of Nt-arginylated substrates exposing Nt-Arg. Our results suggest that p62 acts as a general adaptor for Nt-Arg of various Nt-arginylated proteins and peptides (Fig. 4) and that the Nt-Arg residues of arginylated substrates represent a proteome that modulates macroautophagy through p62 and possibly other autophagic adaptors. Through this global mechanism, cells can sense and react to accumulating autophagic cargoes by activating macroautophagy in a timely fashion.

Studies have shown that Nt-arginylation generates an N-degron that induces proteolysis of short-lived regulators via the UPS (5). In principle, five (Asn, Gln, Cys, Asp, and Glu) of 20 principal amino acids can induce proteasomal degradation through Nt-arginylation, representing almost 25% of proteolytic cleavage products. It has been a mystery, however, why only a handful of mammalian proteins are known to be degraded through arginylation (15). In addition, it has been observed for several decades that many proteins harboring the Nt-Arg are not degraded by the N-end rule pathway (25–27). This paradoxical scarceness of its physiological substrates suggests that the major functions of Nt-arginylation may not be confined to selective proteolysis of short-lived regulators through the UPS. Our results reconcile the studies that characterized arginylation in proteasomal degradation with those that consistently reported lack of degradation of arginylated proteins (25–27).

Materials and Methods

Cell culture, immunoblotting, plasmids, reagents, antibodies, dot blotting, peptide-binding/competition assays, protein degradation assays, immunocytochemistry, in vitro p62 oligomerization assays, immunoprecipitation assays, and immunohistochemistry were performed using standard techniques, which are described in *SI Materials and Methods*.

Animal studies were conducted according to the *Guide for the Care and Use of Laboratory Animals* (28) and the protocols (SNU130604) approved by the Institutional Animal Care and Use Committee at Seoul National University.

ACKNOWLEDGMENTS. We thank Hyunjoo Cha-Molstad for critical advice during early studies and Sung Tae Kim for critical advice and experimental guidance. This work was funded by the Basic Science Research Programs of the National Research Foundation (NRF) funded by the The Ministry of Science, ICT and Future Planning (MSIP) (NRF-2016R1A2B3011389 to Y.T.K.), the Brain Korea 21 PLUS Program [to Seoul National University (SNU)], the SNU Nobel Laureates Invitation Program (A.C.), Israel Science Foundation (ISF) (A.C.), The German Israeli Foundation for Research and Development (GIF) (A.C.), the Israel Centers of Research Excellence (I-CORE) Program of the Planning and Budgeting Committee and ISF Grant 1775/12 (to A.C.), the Dr. Miriam and Sheldon G. Adelson Medical Research Foundation (A.C.), the R&D Convergence Program (CAP-16-03-KRIBB to B.Y.K.) funded by the National Research Council of Science & Technology and KRIBB Initiative Program, the Bio and Medical Technology Development Program (Project 2012M3A9B6055305) through the Korean Ministry of Education, Science, and Technology, and NIH Grants R21HL1096541 (to X.-Q.X.) and P30 DA035778A1 (to X.-Q.X.). A.C. is an Israel Cancer Research Fund (ICRF) USA Professor.

1. Ciechanover A, Kwon YT (2015) Degradation of misfolded proteins in neurodegenerative diseases: Therapeutic targets and strategies. *Exp Mol Med* 47:e147.
2. Ciechanover A, Kwon YT (2017) Protein quality control by molecular chaperones in neurodegeneration. *Front Neurosci* 11:185.
3. Deng Z, et al. (2017) Autophagy receptors and neurodegenerative diseases. *Trends Cell Biol* 27:491–504.
4. Cha-Molstad H, et al. (2015) Amino-terminal arginylation targets endoplasmic reticulum chaperone BiP for autophagy through p62 binding. *Nat Cell Biol* 17:917–929.
5. Tasaki T, Sriram SM, Park KS, Kwon YT (2012) The N-end rule pathway. *Annu Rev Biochem* 81:261–289.
6. Kwon YT, Kashina AS, Varshavsky A (1999) Alternative splicing results in differential expression, activity, and localization of the two forms of arginyl-tRNA-protein transferase, a component of the N-end rule pathway. *Mol Cell Biol* 19:182–193.
7. Tasaki T, et al. (2005) A family of mammalian E3 ubiquitin ligases that contain the UBR box motif and recognize N-degrons. *Mol Cell Biol* 25:7120–7136.
8. Sriram SM, Kim BY, Kwon YT (2011) The N-end rule pathway: Emerging functions and molecular principles of substrate recognition. *Nat Rev Mol Cell Biol* 12:735–747.
9. Turk B (2006) Targeting proteases: Successes, failures and future prospects. *Nat Rev Drug Discov* 5:785–799.
10. Crawford ED, Wells JA (2011) Caspase substrates and cellular remodeling. *Annu Rev Biochem* 80:1055–1087.
11. Bachmair A, Finley D, Varshavsky A (1986) In vivo half-life of a protein is a function of its amino-terminal residue. *Science* 234:179–186.
12. Piatkov KI, Oh JH, Liu Y, Varshavsky A (2014) Calpain-generated natural protein fragments as short-lived substrates of the N-end rule pathway. *Proc Natl Acad Sci USA* 111:E817–E826.
13. Varshavsky A (2012) Augmented generation of protein fragments during wakefulness as the molecular cause of sleep: A hypothesis. *Protein Sci* 21:1634–1661.
14. Decca MB, et al. (2007) Post-translational arginylation of calreticulin: A new isospecies of calreticulin component of stress granules. *J Biol Chem* 282:8237–8245.
15. Lee MJ, et al. (2005) RGS4 and RGS5 are in vivo substrates of the N-end rule pathway. *Proc Natl Acad Sci USA* 102:15030–15035.
16. Petersen BO, et al. (2000) Cell cycle- and cell growth-regulated proteolysis of mammalian CDC6 is dependent on APC-CDH1. *Genes Dev* 14:2330–2343.
17. Cha-Molstad H, et al. (2017) p62/SQSTM1/Sequestosome-1 is an N-recognin of the N-end rule pathway which modulates autophagosome biogenesis. *Nat Commun* 8:102.
18. Piatkov KI, Brower CS, Varshavsky A (2012) The N-end rule pathway counteracts cell death by destroying proapoptotic protein fragments. *Proc Natl Acad Sci USA* 109: E1839–E1847.
19. Xu Z, Payoe R, Fahlman RP (2012) The C-terminal proteolytic fragment of the breast cancer susceptibility type 1 protein (BRCA1) is degraded by the N-end rule pathway. *J Biol Chem* 287:7495–7502.
20. Brower CS, Piatkov KI, Varshavsky A (2013) Neurodegeneration-associated protein fragments as short-lived substrates of the N-end rule pathway. *Mol Cell* 50:161–171.
21. Kwon YT, et al. (2002) An essential role of N-terminal arginylation in cardiovascular development. *Science* 297:96–99.
22. Salomons FA, et al. (2009) Selective accumulation of aggregation-prone proteasome substrates in response to proteotoxic stress. *Mol Cell Biol* 29:1774–1785.
23. Vivès E, Brodin P, Lebleu B (1997) A truncated HIV-1 Tat protein basic domain rapidly translocates through the plasma membrane and accumulates in the cell nucleus. *J Biol Chem* 272:16010–16017.
24. Lee DH, et al. (2016) TRAIL-induced caspase activation is a prerequisite for activation of the endoplasmic reticulum stress-induced signal transduction pathways. *J Cell Biochem* 117:1078–1091.
25. Cornachione AS, et al. (2014) Arginylation of myosin heavy chain regulates skeletal muscle strength. *Cell Rep* 8:470–476.
26. Karakozova M, et al. (2006) Arginylation of beta-actin regulates actin cytoskeleton and cell motility. *Science* 313:192–196.
27. Wang J, et al. (2017) Arginyltransferase ATE1 is targeted to the neuronal growth cones and regulates neurite outgrowth during brain development. *Dev Biol* 430: 41–51.
28. National Research Council (1996) *Guide for the Care and Use of Laboratory Animals* (National Academies Press, Washington, DC), 7th Ed.